IEEE Access
Multidisciplinary ⋮ Rapid Review ⋮ Open Access Journal

Received January 22, 2021, accepted February 4, 2021, date of publication February 15, 2021, date of current version February 26, 2021.

Digital Object Identifier 10.1109/ACCESS.2021.3059522

A Robust Sparse RLS-Volterra Nonlinear Equalizer Using ℓ_0-Regularization for 4 × 150 Gbit/s IMDD-Based Optical Interconnect

WEN CHENG, HAIPING SONG, DI LI, PIN YI, MENGFAN CHENG, DEMING LIU, AND LEI DENG

Wuhan National Laboratory for Optoelectronics, School of Optical and Electronic Information, Huazhong University of Science and Technology (HUST), Wuhan 430074, China

Corresponding author: Lei Deng (denglei_hust@mail.hust.edu.cn)

This work was supported in part by the National Key Research and Development Program of China under Grant 2018YFB1800903, in part by the National Natural Science Foundation of China under Grant 61675083, and in part by the Fundamental Research Funds for Central Universities HUST under Grant 2019kfyXMBZ033.

ABSTRACT Volterra equalizer (VE) is a well-known and effective algorithm to deal with the linear and nonlinear distortions in optical interconnect, but the high computational complexity hinders its practical application. Generally, sparse VEs based on ℓ_1- or ℓ_0-regularization are good ways to reduce the complexity by discarding some inessential taps. However, a tap threshold needs to be chosen in these sparse VEs like the threshold-based pruned retraining VE (TR-VE) to decide the discarded taps. And this tap threshold should be adjusted fine to balance the reduced complexity and equalization performance, especially when the testing environments alter. Thus, the reduced complexity in these sparse VEs may fluctuate. To address this issue, a robust and stable complexity reduced sparse VE using ℓ_0-regularization (ℓ_0-SR-VE) is proposed in this paper. The recursive least square (RLS) algorithm is used to replace the least mean square algorithm for the faster convergence speed and better equalization performance. The complexity of this equalizer depends on its parameters but not the tap threshold. Once the equalizer parameters are determined, the complexity would not change with the system characteristics, contributing to higher practicability. In our experiment, a 150 Gbit/s PAM8 signal transmission system based on intensity modulation and direct detection (IMDD) is achieved, and a dual-drive Mach-Zehnder modulator for optical single-sideband signal generation is used to mitigate the power fading effect. The experimental results show that with the help of ℓ_0-SR-VE, the reduced complexity percentage is stable at 66.18% compared with the RLS-based VE, even after 75 km standard single-mode fiber (SSMF) transmission. By using this equalizer, 4 × 150 Gbit/s PAM8 signals have also been successfully transmitted over 30 km SSMF at C-band. The reduced complexity variation of ℓ_0-TR-VE is >20%, but the reduced complexity of the proposed ℓ_0-SR-VE is stable at 60% even after 30 km SSMF for all four lanes.

INDEX TERMS PAM8, IMDD system, data center interconnect (DCI), sparse Volterra equalizer (VE).

I. INTRODUCTION

Driven by the diverse new applications such as the 5th generation (5G) mobile communication, virtual reality, and cloud computing, high-capacity data center interconnect (DCI) with simple structure and low cost is highly desired. The combination of intensity modulation and direct detection (IMDD) system and 4-level pulse amplitude modulation (PAM4) format is an attractive solution for DCI by considering power consumption, transmission performance, and complexity of transceivers. DCI still faces an urgent requirement in capacity even though the data rate per lane has evolved from 25 Gbit/s to the current 100 Gbit/s [1], [2]. To further increase the transmission capacity under the condition of

The associate editor coordinating the review of this manuscript and approving it for publication was Maged Abdullah Esmail.

current bandwidth-limited components, PAM8 with high spectrum efficiency would be a good candidate. In recent years, many schemes based on PAM8 have been reported for the realization of >100 Gbit/s per wavelength [3], [4]. Moreover, optical single sideband (SSB) modulation is proved to be effective to overcome the chromatic dispersion (CD) induced power fading effect, contributing to large-scale optical interconnections. To generate an optical SSB signal, a dual-drive Mach-Zehnder modulator (DDMZM) is more attractive in IMDD systems compared with a dual-parallel modulator (DPMZM) due to its low cost [5]–[8].

Generally, to combat the linear and nonlinear distortions such as signal-to-signal beat interference (SSBI) in a typical IMDD system, feed-forward equalizer (FFE), Kramers-Kronig (KK) algorithm, iterative cancellation (IC) algorithm, and Volterra equalizer (VE) are commonly used in the receiver. Compared with FFE, VE can cope with linear and nonlinear impairments simultaneously [1]. For example, in a 112 Gbit/s PAM4 short reach transmission using a directly modulated laser [1], a three-order VE is used for nonlinear post-compensation. By using the proposed tap coefficient decision-directed VE, 180 Gbit/s PAM8 signals are successfully transmitted over 2 km standard single-mode fiber (SSMF) in an IMDD system with 10-dB bandwidth of 17.5 GHz [9]. On the other hand, the IC algorithm treats the SSBI term as a perturbation to be calculated and subtracted [10]. In contrast, the KK receiver eliminates the SSBI by accurately reconstructing the complex field of the transmitted SSB signal [10], thus the KK algorithm usually outperforms the IC algorithm as reported in [10], [11]. Nonetheless, the KK algorithm faces challenges of high complexity and high up-sampling factor [12], and a two-order VE is proved to have better bit error rate (BER) performance than the combination of KK algorithm and FFE after 80 km SSMF transmission as reported in [8]. Therefore, the VE algorithm has a promising prospect in the future cost-constrained high-speed optical transmission system.

Unfortunately, the computational complexity of VE grows exponentially with the increase of the memory length, which hinders the practical application to a power-sensitive optical interconnection system based on IMDD. To overcome this problem, several methods have been proposed to reduce the complexity with the main idea of discarding inessential taps. Generally, these methods can be divided into two categories. Firstly, a simplified VE with a special structure is formed by selecting fixed taps from a full VE. For example, a reduced-complexity scheme is presented in [13] for the two-order Volterra nonlinear equalizer (R2-VNLE), in which the number of signals beating terms in the nonlinear part is limited. Especially, only the coefficients on the diagonal are reserved, and this is the simplest case of R2-VNLE [14]. Secondly, a sparse VE is constructed by discarding some inessential taps dynamically according to the absolute value of these taps. For instance, the threshold-based pruned retraining VE (TR-VE) is proposed in [15], and ℓ_1-regularization is used to optimize the threshold selection. In [16], a Volterra filter based on least mean squares (LMS) algorithm is used in a 112 Gbit/s PAM4 transmission system, and experimental results show that ℓ_0-regularization achieves lower complexity and more precise weights compared to ℓ_1-regularization. Overall, the first category method does not consider the real system characteristic, and it is bound to sacrifice the equalization performance. The second category method could be adaptive to different systems, realizing the best performance according to the different system characteristics.

The reported sparse Volterra equalizers above are mostly based on LMS [13]–[16]. We all know that the recursive least square (RLS) algorithm has a faster convergence speed and lower mean square error than LMS, and thus it has been used in a sparse RLS-based VE using ℓ_1-regularization in our previous work [17]. To further reduce the algorithm complexity, it is meaningful to introduce the ℓ_0-regularization to the RLS-based VE considering that ℓ_0-regularization outperforms ℓ_1-regularization. Besides, the robustness of the used equalizer also needs to be considered in practice. For example, the reduced complexity percentage of TR-VE is sensitive to the chosen tap threshold because tap coefficients would be varied as the testing environments change. To avoid these problems, we propose a robust and stable complexity reduced sparse RLS-based Volterra nonlinear equalizer (SR-VE) using ℓ_0-regularization in this paper for the first time, and the complexity of this equalizer depends on its parameters but not the tap threshold. Once the equalizer parameters are determined, the complexity would not change with the system characteristics, contributing to higher practicability. In our experiment, SR-VE, SR-VE using ℓ_0-regularization (ℓ_0-SR-VE), and ℓ_1-regularization (ℓ_1-SR-VE) are all analyzed and compared, and the ℓ_0-SR-VE is proven to be the best choice.

By using the proposed ℓ_0-SR-VE, 150 Gbit/s PAM8 signal transmission over 40 km SSMF is successfully achieved at C-band, and no CD compensation technique is required due to the use of DDMZM and optical SSB modulation. Experimental results show that compared to the RLS-based VE, the proposed ℓ_0-SR-VE has lower complexity, and the maximum complexity reduction percentage at the 7% hard-decision forward error correction (HD-FEC) threshold with BER of 3.8×10^{-3} is up to 66.18% for OB2B and 40 km SSMF transmission. Furthermore, we extend our previous work in [18] and experimentally demonstrate transmission of 4 × 150 Gbit/s PAM8 signal over 30 km SSMF at C-band by using the proposed ℓ_0-SR-VE.

II. PRINCIPLE

A. SPARSE SYSTEM IDENTIFICATION

System identification is the opposite operation of channel equalization. The equalization performance is following the accuracy of the system identification. In this section, we analyze the accuracy of different system identification algorithms including LMS, RLS, and their variants by simulation. According to [19], the system identification based on LMS

with convex regularization can be expressed as:

$$\begin{aligned} e(n) &= d(n) - w^T(n-1)\,x(n), \\ w(n) &= w(n-1) + \mu e(n)\,x(n) - \mu\gamma\nabla^S f(w(n-1)), \end{aligned} \tag{1}$$

and the system identification based on RLS with convex regularization [20] can be described as:

$$\begin{aligned} e(n) &= d(n) - w^T(n-1)\,x(n), \\ k(n) &= \frac{P(n-1)\,x(n)}{\lambda + x^T(n)\,P(n-1)\,x(n)}, \\ P(n) &= \frac{1}{\lambda}\left[P(n-1) - k(n)\,x^T(n)\,P^T(n-1)\right], \\ w(n) &= w(n-1) + k(n)\,e(n) \\ &\quad - \gamma(1-\lambda)\,P(n)\,\nabla^S f(w(n-1)), \end{aligned} \tag{2}$$

where $d(n)$ denotes the desired sample, $x(n)$ and $w^T(n-1)$ represents the input vector and weight vector, respectively. $e(n)$ is the estimation error of the adaptive algorithm, and μ is the step-size of the LMS algorithm. $\gamma > 0$ is the regularization parameter that governs the tradeoff between the sparsity and the estimation error. $\nabla^S f(w(n-1))$ is the subdifferential of $f(w(n-1))$, and $f(w(n-1))$ means the ℓ_0 norm or ℓ_1 norm of $w(n-1)$. $P(0) = k_p \cdot I_N$, here k_p is a positive constant and I_N is identity matrix. $k(n)$ and $P(n)$ are the n-th order iterative value, and λ is the forgetting factor.

Generally, ℓ_0 norm is approximated by a continuous function. A popular approximation reported in [19] could be expressed as:

$$\begin{aligned} f(w) &= \|w\|_0 \approx f^\beta(w) = \sum_{i=0}^{N-1}\left(1 - e^{-\beta|w_i|}\right), \\ \nabla^S f^\beta(w_i) &= \beta\,\mathrm{sgn}(w_i)\,e^{-\beta|w_i|}. \end{aligned} \tag{3}$$

By using Taylor series expansions of the exponential function, we can get

$$e^{-\beta|w_i|} = \begin{cases} e^{-\beta w_i}, & w_i \geq 0 \\ e^{\beta w_i}, & w_i < 0 \end{cases} \approx \begin{cases} 1 - \beta w_i, & |w_i| \leq \dfrac{1}{\beta} \\ 0, & elsewhere, \end{cases} \tag{4}$$

then

$$\nabla^S f^\beta(w_i) \approx \begin{cases} \beta\,\mathrm{sgn}(w_i) - \beta^2 w_i, & |w_i| \leq \dfrac{1}{\beta} \\ 0, & elsewhere, \end{cases} \tag{5}$$

where β is an appropriate positive constant.

For ℓ_1 norm, we have

$$\begin{aligned} f(w) &= \|w\|_1 = \sum_{i=0}^{N-1}|w_i|, \\ \nabla^S f(w_i) &= \mathrm{sgn}(w_i). \end{aligned} \tag{6}$$

For simplicity, when $\gamma = 0$, the above algorithm is defined as LMS/RLS. When $\gamma \neq 0$ and $f(w) = \|w\|_0$, the above algorithm is defined as ℓ_0-LMS/RLS.

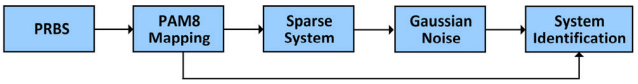

FIGURE 1. The process of the sparse system identification.

When $\gamma \neq 0$ and $f(w) = \|w\|_1$, the above algorithm is defined as ℓ_1-LMS/RLS. And oracle-LMS/RLS is the LMS/RLS algorithm in which the positions of the nonzero taps are known in advance.

To compare the accuracy of different system identification algorithms, we have built up a simulation system based on MATLAB as shown in Fig. 1. A pseudorandom bit sequence (PRBS) with a length of 2^{15}-1 is used for bit-to-PAM8 symbol mapping. Subsequently, the PAM8 signal passes through a sparse system with Gaussian noise. Finally, the sparse system identification is performed using different algorithms including RLS/LMS, oracle-RLS/LMS, ℓ_0-RLS/LMS, and ℓ_1-RLS/LMS. The transmitted PAM8 signal is used as a training sequence at this stage.

In our simulation, the total tap number of the sparse system w is $N = 64$, where only 8 taps of them are nonzero. The nonzero taps are positioned randomly and their values are taken from a normal distribution $N(0, 1)$. The signal-to-noise ratio (SNR) is set as 25 dB. For a fair comparison, all parameters are optimally selected. $\mu = 10^{-4}$, k_p is set to 1, and $\lambda = 0.9996$. γ for LMS and RLS are set to 0.03 and 30 respectively, and β is 50. The impulse response of this sparse system is shown in Fig. 2(a). Fig. 2(b) shows the variation of the mean square deviations (MSD) versus iteration number, and the MSD is calculated as:

$$MSD = 10\log_{10}\left(\|w - w(n)\|_2^2\right), \tag{7}$$

where w is the impulse response of this sparse system, $w(n)$ is the estimated value of the sparse system at the time of n, and $\|\cdot\|_2$ is ℓ_2 norm of the vector.

It can be observed that oracle-RLS/LMS has the best performance because the positions of the zero taps are known in advance. RLS/LMS using convex regularization has better system identification accuracy than RLS/LMS, because ℓ_0 and ℓ_1 norm perform zero-point attraction to small adaptive taps [19], this result is consistent with the simulation results in [20]. Moreover, ℓ_0-RLS/LMS has better performance than ℓ_1-RLS/LMS. Not only the convergence speed of the RLS algorithm is faster than the LMS algorithm, but also the MSD of the RLS algorithm is lower than that of the LMS algorithm. In general, the MSD of ℓ_0-RLS is very close to that of oracle-RLS, which means a nice equalization performance for the equalizers using the ℓ_0-RLS algorithm.

B. SPARSE VOLTERRA EQUALIZER

As mentioned above, the computational complexity of a full VE will be extremely high when the number of kernels and their corresponding memory length is increased. The relationship between the computational complexity and the memory length can be found in [13]. Generally, a three-order VE is sufficient to compensate for linear and

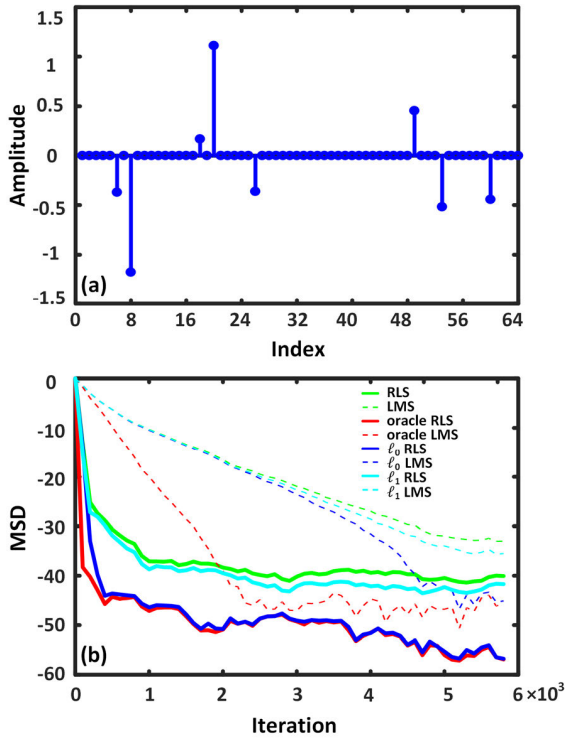

FIGURE 2. The impulse response of the sparse system (a). The MSD of different sparse system identification algorithms (b).

nonlinear impairments [21]. For simplicity, a three-order VE with memory length of l_1, l_2 and l_3 is denoted as VE(l_1, l_2, l_3). As described in our previous work [17], a full VE has many insignificant taps and these insignificant taps could be discarded to reduce the computational complexity without equalization performance degradation. As described in Section I, the TR-VE algorithm reported in [15] is a good way to reduce the complexity of VE, and this idea is to tune the threshold T_k to determine which taps to be cut off. Therefore, the reduced algorithm complexity depends on the threshold T_k. T_k is set for different orders and it can be described as $w_{m_1,\ldots,m_k} = 0$, if $w_{m_1,\ldots,m_k} < T_k$. However, the tap coefficients will vary with the testing environments, and thus the optimum value of T_k is not constant. In other words, the reduced algorithm complexity will fluctuate at a fixed T_k value when the testing environments such as the received optical power (ROP) at the receiver is changed, resulting in the loss of practicality.

To address this issue, we have proposed a robust and stable complexity reduced sparse RLS-based VE as shown in Fig. 3. As mentioned in section II.A, the ℓ_0-RLS algorithm has the best MSD performance when the positions of the nonzero taps are unknown. Therefore, it's meaningful to introduce the ℓ_0-regularization to the proposed SR-VE to achieve the maximum complexity reduction at the same BER performance. For an RLS-based VE (RLS-VE), the cost function can be written as

$$J(n) = \frac{1}{2}|d(n) - y(n)|^2, \tag{8}$$

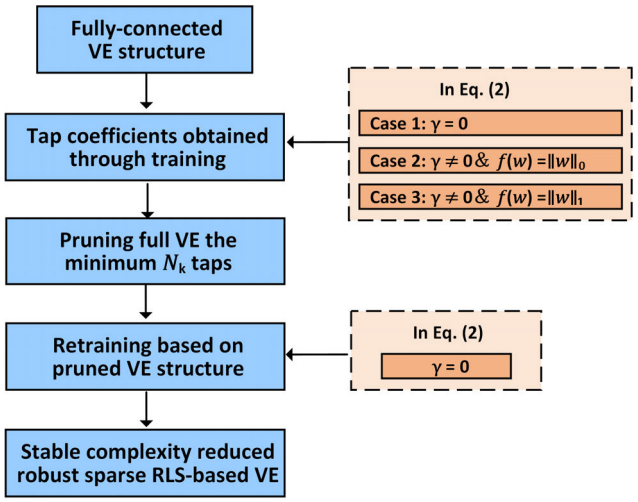

FIGURE 3. The principle of the proposed robust and stable complexity reduced sparse RLS-based VE.

where $d(n)$ is the training symbol, and $y(n)$ is the output signal of VE. To reduce the algorithm complexity as much as possible, the ℓ_0- or ℓ_1-regularization is introduced into the RLS algorithm, and then the cost function can be rewritten as

$$J(n) = \frac{1}{2}|d(n) - y(n)|^2 + \gamma \|w(n)\|_0, \tag{9}$$

or

$$J(n) = \frac{1}{2}|d(n) - y(n)|^2 + \gamma \|w(n)\|_1, \tag{10}$$

the last term in Eq. (9) and (10) are the penalty term of ℓ_0 and ℓ_1 norm, respectively. Compared to Eq. (8), these penalty terms in Eq. (9) and (10) can shrink more tap coefficients close to zero. In our scheme, the RLS algorithm is used to update the tap coefficients of VE, and the updating process can be described as Eq. (2). Noted that different from the sparse system identification process, in the equalization process, $d(n)$ denotes the training symbol, $x(n)$ and $w^T(n-1)$ represents the input vector and tap coefficient of VE, respectively.

The operation principle of the proposed SR-VE is shown in Fig. 3, and a full RLS-VE is obtained according to Eq. (2). At the step of the training process, three kinds of SR-VE algorithms named SR-VE, ℓ_0-SR-VE, and ℓ_1-SR-VE are used. Subsequently, this full RLS-VE is pruned by cutting off the minimum N_k taps. The equalization performance will deteriorate rapidly in this case. Therefore, it is necessary to retrain the tap coefficients by using Eq. (2) in which $\gamma = 0$. The algorithm complexity in the equalization processing of a full VE and the proposed SR-VE can be calculated as:

$$\begin{aligned} M_1 &= l_1 \\ M_2 &= \frac{1}{2} l_2 (l_2 + 1) \\ M_3 &= \frac{1}{2}[1 \times (1+1) + 2 \times (2+2) + \ldots + l_3 \times (l_3 + 1)] \\ C_1 &= M_1 + 2M_2 + 3M_3 \\ C_2 &= M_1 + 2(M_2 - N_2) + 3(M_3 - N_3), \end{aligned} \tag{11}$$

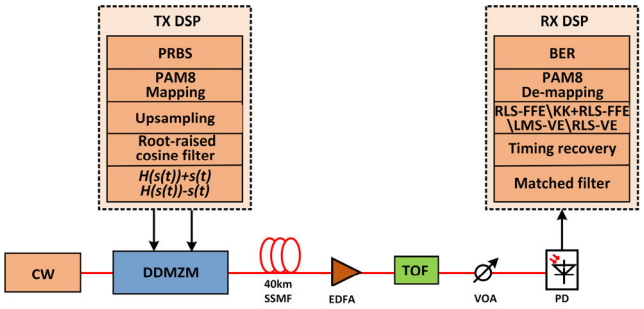

FIGURE 4. The simulation setup of 150 Gbit/s PAM8 signal over 40 km SSMF transmission.

where M_1, M_2 and M_3 are the number of taps of the r-th order kernel. N_2 and N_3 are the number of taps to be discarded in the k-th order kernel. C_1 and C_2 represent the computational complexity of the full VE and the proposed SR-VE, respectively. Not the threshold but the optimized parameters N_2 and N_3 are used for pruning in the proposed SR-VE. Obviously, C_2 only depends on l_1, l_2, l_3, N_2 and N_3, thus the complexity of this equalizer only depends on its parameters. Once the parameters of this equalizer are determined, the complexity would not change with the testing environments, contributing to higher practicability. It could be observed that the reduced complexity percentage with the help of SR-VE can be expressed as

$$P = 1 - \frac{C_2}{C_1}. \tag{12}$$

III. SIMULATION SETUP AND RESULTS

To analyze the transmission performance of RLS-FFE, KK algorithm with RLS-FFE, LMS-VE, and RLS-VE, a joint simulation setup based on VPI Transmission Maker 9.9 and MATLAB is built up as shown in Fig. 4. It has been proven in our previous work [17] that DDMZM-based SSB modulation can effectively eliminate the power fading effect. At the transmitter, a PRBS with a length of 2^{15}-1 is used for PAM8 symbol mapping. The generated 50 GBaud PAM8 signals are up-sampled by inserting one zero between every two symbols, thus the sampling rate after up-sampling is 100 GSa/s. Subsequently, this up-sampled PAM8 signal is pulse-shaped by a root-raised cosine with a roll-off of 0.1. The generated driving signal for each input port of DDMZM is adjusted to $I(t) = H(s(t)) + s(t)$ and $Q(t) = H(s(t)) - s(t)$ for SSB modulation, here $s(t)$ and $H(s(t))$ corresponds to the PAM8 signal and its Hilbert transformation respectively. The driving signal $I(t)$ and $Q(t)$ are then filtered by an electrical low pass filter (LPF) with a 4-order Bessel model to emulate the bandwidth-limited system. The filtered $I(t)$ and $Q(t)$ are used to drive a DDMZM biased at its quadrature point. The half-wave voltage of this DDMZM is set as 1.8 V. A 100 kHz-linewidth continuous-wave (CW) with a frequency of 193.1 THz is served as the optical source.

After 40 km SSMF propagation, the optical signal is first amplified by an Erbium-doped optical fiber amplifier (EDFA), and a tunable optical filter (TOF) is then used to remove the out-of-band noise and the residual sideband. A variable optical attenuator (VOA) is placed after TOF for receiver sensitivity measurement. Finally, the received signal is detected by a photodetector (PD). The received electrical signal is sent to MATLAB for performance evaluation. In the receiver digital signal processing (DSP), the received signal is passed through a matched filter which is the same as the shaping filter at the transmitter. A timing recovery procedure is used to remove the timing offset and jitter from the received signal. Several equalization algorithms including RLS-FFE, the conventional KK algorithm with RLS-FFE, LMS-VE, and RLS-VE are used to cope with the nonideal distortions. After the symbol-to-bit de-mapping, BER performance is calculated.

TABLE 1. The computational complexity and the equalization performance of LMS-VE, ℓ_0-SL-VE, RLS-VE, and ℓ_0-SR-VE.

Algorithms	Computational Complexity	-$\log_{10}$(BER)
LMS-VE	2125	2.297
ℓ_0-SL-VE	625	2.25
RLS-VE	2125	2.76
ℓ_0-SR-VE	625	2.74

We first scan the amplitude of the driving signal to find the optimal peak-to-peak voltage (Vpp) for different DSP algorithms. Fig. 5 shows the measured BER performance of RLS-FFE, the conventional KK algorithm with RLS-FFE, LMS-VE, and RLS-VE in terms of different Vpp values at the ROP of 0 dBm after 40 km SSMF transmission. By considering the tradeoff between equalization performance and computational complexity [9], the memory length of FFE and VE is set to (55) and (55,45,0), respectively. The sampling rate of the KK algorithm is set to 6 samples per symbol [12]. It can be seen in Fig. 5 that when the Vpp value is lower than 0.4 V, the measured BER performance is similar in all kinds of equalization algorithms, and it could be attributed to that the AWGN noise is the major limiting factor in this case. By accurately reconstructing the complex field for SSBI elimination, the KK algorithm is helpful to increase the transmission performance when RLS-FFE is used [7]. Due to the impact of the severe nonlinear effect, the achieved BER performance by using KK and RLS-FFE still cannot reach the HD-FEC threshold. By introducing VE which could handle the linear and nonlinear distortions simultaneously, the transmission performance could be further improved. The measured BER performance could go below the HD-FEC limit when RLS-VE (55,45,0) is used, but the computational complexity of VE can be very high with the increase of the memory length. Therefore, it is highly desired to reduce the algorithm complexity.

Generally, the complexity calculation methods for LMS-VE and RLS-VE are the same, as well as the robust and stable complexity reduced sparse LMS-based Volterra

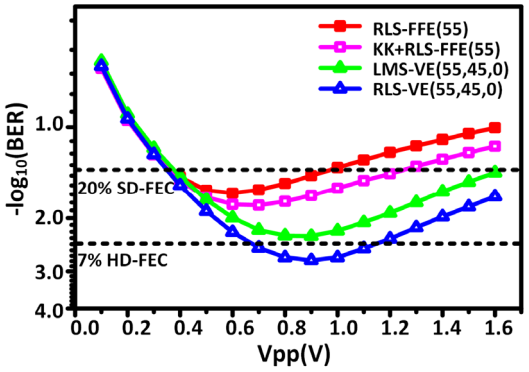

FIGURE 5. The measured BER performances of 150 Gbit/s PAM8 signal over 40 km SSMF transmission using DSP algorithms in terms of the Vpp of the driving signal.

nonlinear equalizer (ℓ_0-SL-VE), and the ℓ_0-SR-VE. And their complexities could all be calculated by Eq. (11). Table 1 shows the computational complexity and the measured equalization performance of LMS-VE, RLS-VE, ℓ_0-SL-VE, and ℓ_0-SR-VE at the Vpp value of 0.9 V. In this test, l_1, l_2, l_3, N_2, and N_3 are set to 55, 45, 0, 750, and 0, respectively. It can be seen that ℓ_0-SL-VE and ℓ_0-SR-VE are effective to reduce the computational complexity by 70% with negligible equalization performance degradation, compared to LMS-VE and RLS-VE, respectively.

Fig. 6(a) shows the normalized tap coefficient of the second-order kernel in terms of the n_2-th smallest tap of RLS-VE (55,45,0) under different ROP values, and the Vpp of the driving signal is 0.9 V. The normalized tap coefficient is defined as the ratio of the tap coefficient of the k-th order kernel to the maximum tap coefficient of the k-th order kernel. Obviously, the smaller the normalized tap coefficient is, the less important the tap is, and thus discarding this tap has less effect on the equalization performance. It is observed in Fig. 6(a) that the second- order normalized tap coefficient varies as the ROP values change. When the TR-VE in [15] is used, the optimum value of the threshold T_k will not be constant because the tap coefficients vary with the ROP, resulting in the fluctuation of the reduced algorithm complexity.

To verify the advantages of the proposed ℓ_0-SR-VE algorithm, the BER performance of 150 Gbit/s PAM8 signal over 40 km SSMF transmission and the reduced complexity percentage using different equalizers in terms of ROP are measured and plotted in Fig. 6(b). In our simulation, the RLS-VE, ℓ_0-SR-VE, and TR-VE with ℓ_0-regularization (ℓ_0-TR-VE) are all tested and compared. Note that the optimum N_k value of ℓ_0-SR-VE and the optimum T_k value of ℓ_0-TR-VE is first obtained at the ROP of 0 dBm, and these two parameters remain unchanged in the rest of the tests. It could be seen that RLS-VE, ℓ_0-SR-VE, and ℓ_0-TR-VE has almost the same equalization performance. Whereas, the computational complexity of ℓ_0-SR-VE and ℓ_0-TR-VE are dramatically decreased compared to the RLS-VE. The reduced complexity percentage using ℓ_0-TR-VE is varied for different ROP, and the variation is over 11%. However, with the help of ℓ_0-SR-VE, the reduced complexity percentage is more stable when the ROP is changed.

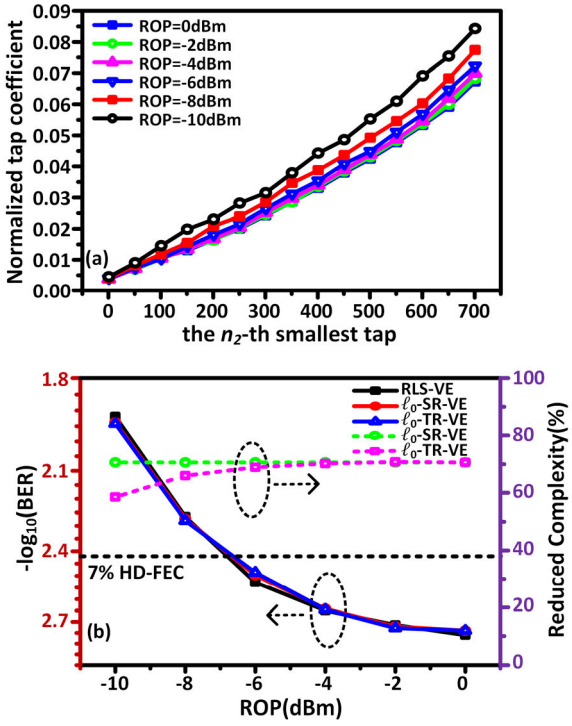

FIGURE 6. The normalized tap coefficient versus the n_2-th smallest tap of the second order kernel under different ROP values at PD (a), the BER performance of 150 Gbit/s PAM8 signal over 40 km SSMF transmission and the reduced complexity percentage using different equalizers in terms of ROP at PD (b).

IV. EXPERIMENTAL SETUP AND DISCUSSIONS

A. SINGLE-CHANNEL 150 GBIT/S PAM8 SIGNAL TRANSMISSION OVER 40 KM SSMF USING THE PROPOSED SR-VE ALGORITHM

Fig. 7 shows the experimental setup of 150 Gbit/s PAM8 signal transmission over 40 km SSMF based on DDMZM. The way to generate driving signal $I(t)$ and $Q(t)$ is the same as the simulation mentioned in Section III. Subsequently, $I(t)$ and $Q(t)$ are both resampled to 64 GSa/s, and they are loaded into an arbitrary waveform generator (AWG, Keysight M8195A). Finally, the resampled $I(t)$ and $Q(t)$ with the optimal Vpp of 1 V are loaded to drive a DDMZM (Fujitsu, FTM7937EZ) biased at its quadrature point. The half-wave voltage of this DDMZM is 1.8 V. Insert (i) of Fig. 7 shows the optical spectrum of the transmitted optical signal after DDMZM. A 100 kHz-linewidth continuous-wave (CW) from an external cavity laser (ECL) with a wavelength of 1550 nm is served as the optical source.

After 40 km SSMF propagation, the optical signal is first amplified by an EDFA, and a TOF (Yenista Optics XTM-50) is then used to remove the out-of-band noise and the residual sideband. Insert (ii) and (iii) of Fig. 7 show the optical spectrum of the signal before and after TOF respectively. A VOA is placed after TOF for receiver sensitivity measurement.

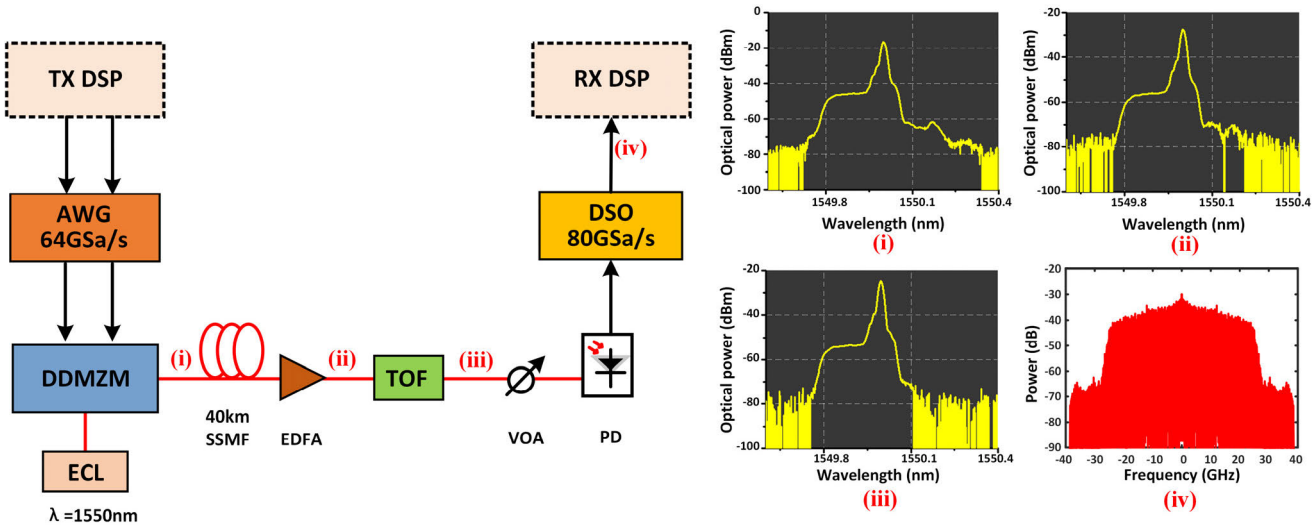

FIGURE 7. The experimental setup of 150 Gbit/s PAM8 signal transmission system using the proposed SR-VE.

Finally, the received signal is detected by a PD, and then it is captured by a digital sampling oscilloscope (DSO, LeCroy LabMaster 10-36Zi-A) operating at 80 GSa/s for the offline process. Insert (iv) of Fig. 7 shows the electrical spectrum of the received signal. In the receiver DSP, the received signal is firstly resampled to 100 GSa/s, and then it is passed through a matched filter. A timing recovery procedure is implemented. A full RLS-VE or sparse VEs is then used to cope with the linear and nonlinear distortions in this transmission system. After the symbol-to-bit de-mapping, BER is counting. In our experiment 32768 symbols are transmitted in a single frame, among them 10000 symbols are used as training symbols and the rest are used as data symbols.

In our experiment, the parameters λ and k_p are optimized according to the equalization performance of the full RLS-based VE, and the optimum value of λ and k_p are 0.99996 and 0.1, respectively. To show the impact of the parameters γ and βon the tap coefficient in our proposed SR-VE algorithms, the normalized tap coefficient of the third-order kernel is tested at a given ROP value of 1 dBm after 40 km SSMF transmission. Subsequently,β and γ are fixed at 50 and 35 respectively, and the normalized tap coefficient of the third-order kernel versus the n_3-th smallest tap is plotted in Fig. 8(a). SR-VE, ℓ_0-SR-VE, and ℓ_1-SR-VE algorithms are all tested and compared. It could be observed that ℓ_0 norm could make most tap coefficients close to zero, contributing to the lowest computational complexity at a given BER value. The impact of the regularization parameter γ and β on the tap coefficients in ℓ_0-SR-VE is also analyzed in our test. Fig. 8(b) shows the normalized tap coefficient in terms of the n_3-th smallest tap of the third order in ℓ_0-SR-VE with different γ values. In this test,β is fixed to 50. Similarly, Fig. 8(c) shows the normalized tap coefficient in terms of the n_3-th smallest tap of the third-order kernel in ℓ_0 -SR-VE with different β values. In this test, γ is fixed 35. It could be observed in Fig. 8(b) and 8(c) that the sparsity of VE is enhanced as the increase of γ and β. The higher the sparsity is, the lower the computational complexity could be, but the more equalization performance degradation will be. Therefore, we need to select the optimum γ, β, N_2 and N_3 to make the computational complexity lowest at a given BER level.

Fig. 9(a) presents the reduced complexity percentage using ℓ_0-SR-VE described in Eq. (12) in terms of different γ. In this test,β is fixed to 50,N_2 and N_3 are scanned to make the computational complexity minimum and the measured BER performance of 150 Gbit/s PAM8 signal over 40 km SSMF transmission better than the HD-FEC limit, and the ROP value is fixed to 1dBm in this test. Note that the memory length of the three-order VE is set to (111,25,13) in this section by considering both the equalization performance and computational complexity. It could be seen that the reduced complexity percentage using ℓ_0-SR-VE can be kept above 62% when the value of γ is in the range of 25 to 45. Similarly, Fig. 9(b) shows the reduced complexity percentage using ℓ_0-SR-VE in terms of different β and γ is fixed to 35 in this test. The reduced complexity percentage using ℓ_0-SR-VE can be kept above 63% when the value of β is in the range of 40 to 110 as shown in Fig. 9(b). Therefore, it is proved that the proposed ℓ_0-SR-VE is robust to these two parameters of γ and β.

Fig. 10(a) and 10(d) shows the measured BER performance of 150 Gbit/s PAM8 signal over OB2B transmission and the reduced complexity percentage using different equalizers in terms of ROP, respectively. The RLS-FFE, full RLS-VE, ℓ_0-TR-VE, ℓ_0-SR-VE, ℓ_1-SR-VE, and SR-VE are all tested and compared. For comparison, the measured BER performance and the reduced complexity percentage of ℓ_0-SR-VE without retraining, ℓ_1-SR-VE without retraining, and SR-VE without retraining are also showed in Fig. 10(a) and 10(d), here the retraining process is the fourth step of our proposed SR-VEs in Fig. 3. It could be seen that the measured BER

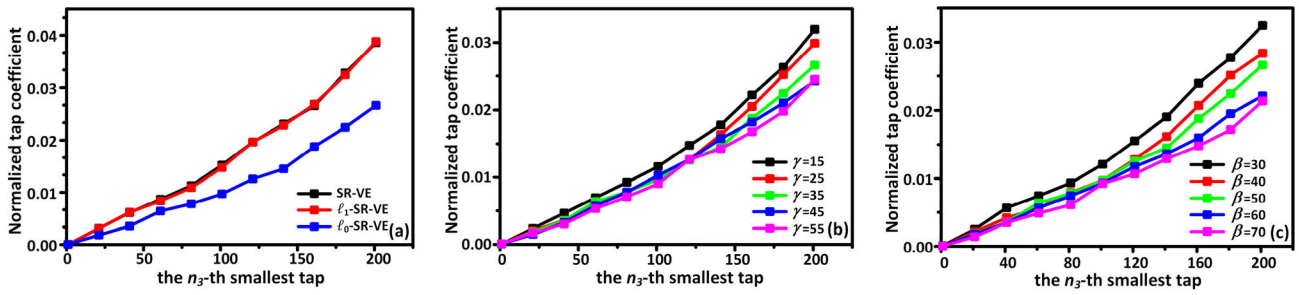

FIGURE 8. The normalized tap coefficient versus the n_3-th smallest tap of the third order in different proposed SR-VEs (a), and in ℓ_0-SR-VE with different γ (b) and β (c).

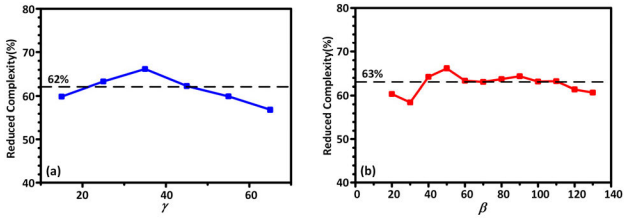

FIGURE 9. The reduced complexity percentage using ℓ_0-SR-VE in terms of different γ (a) and β (b) at the ROP of 1 dBm after OB2B transmission.

value using RLS-FFE of 150 Gbit/s PAM8 signal over OB2B can only below the 20% overhead soft-decision forward error correction (SD-FEC) threshold of 2.0×10^{-2}. ℓ_0-TR-VE, ℓ_0-SR-VE, ℓ_1-SR-VE, and SR-VE have slightly different equalization performance, and a 0.5 dB power penalty is observed compared to the full RLS-VE. It could be seen that the BER performance without retraining is much worse than that with retraining. Specifically, the best BER performance after 40 km SSMF transmission cannot below the HD-FEC threshold. Note that the retraining only needs to be run once at the beginning of equalization, and thus it has little impact on the computational complexity. These results show that the processing of retraining in Fig. 3 is essential and helpful. However, the reduced complexity percentage using ℓ_0-TR-VE is fluctuating for different ROP, and the variation is over 18%. In contrast, the reduced complexity percentage of our proposed three kinds of SR-VEs is stable when the ROP is changed. The complexity of ℓ_1-SR-VE is lower than that of SR-VE, and ℓ_0 -SR-VE has the lowest computational complexity. In this test, we first obtain the optimum N_k value of ℓ_0-SR-VE, ℓ_1-SR-VE, and SR-VE, and the optimum T_k value of ℓ_0-TR-VE. These parameters are determined when the measured BER performance at the ROP of 1 dBm after 40 km SSMF transmission is better than the HD-FEC limit and the computational complexity is the lowest of each nonlinear equalizer. And these optimal parameters are kept unchanged to equalize signals with different ROP or different transmission distances. The same phenomena could be observed in Fig. 10(b) and 10(e) after 40 km SSMF transmission. The reduced complexity percentage variation of ℓ_0-TR-VE is over 11%, and our proposed three kinds of SR-VEs still have stable computational complexity.

To investigate the robustness of the proposed three kinds of SR-VEs, the measured BER performance of 150 Gbit/s PAM8 signal and the reduced complexity percentage using different equalizers in terms of fiber length is measured and plotted in Fig. 10(c) and 10(f). With the increase of fiber length, all the measured BER performance is degraded. This could be attributed to the power fading effect induced by the imperfect SSB modulation and the worsen signal to noise ratio (SNR) as the increase of fiber length. The reduced complexity percentage using ℓ_0-TR-VE changes dramatically, and the reduced complexity percentage variation of ℓ_0-TR-VE is about 44%. It could be observed that with the help of ℓ_0-SR-VE, the reduced complexity percentage is stable at 66.18% even after 75 km SSMF transmission. However, the BER value of 150 Gbit/s PAM8 signal over 65 km SSMF could go below the 20% overhead SD-FEC threshold in our experiment.

B. 4 × 150 GBIT/S PAM8 SIGNAL TRANSMISSION OVER 30 KM SSMF USING THE PROPOSED SR-VE ALGORITHM

To further increase the channel capacity, the experimental demonstration of 4 × 150 Gbit/s PAM8 signal transmission over 30 km SSMF has been built up as shown in Fig. 11. In the transmitter, four ECLs with the wavelength of 1551.6 nm, 1552.4 nm, 1553.2 nm, and 1554.0 nm are used as the optical sources, corresponding to Lane1, Lane2, Lane3, and Lane4, respectively. A four-channel AWG (Keysight M8195A) with a sampling rate of 64 GSa/s is used to generate a four-channel 150 Gbit/s SSB-PAM8 signal as described in Section II.A. The differential output ports of this AWG are also adopted since only one AWG is available in our laboratory. The electrical signal with a peak-to-peak voltage of 1 V from eight output ports of AWG is directly driven to four DDMZMs (Fujitsu, FTM7937EZ) simultaneously. All DDMZMs are biased at their quadrature points, and the half-wave voltage of these DDMZMs is 1.8 V. Note that the generated SSB-PAM8 signal by using the output port CH1 and CH2 of this AWG is delayed to decorrelate with the output signal of CH3 and CH4. Moreover, the output signal of CH1, CH2, and their differential ports are used to modulate the optical sources with a wavelength of 1551.6 nm and 1553.2 nm, respectively. Similarly, the output signal of CH3, CH4, and

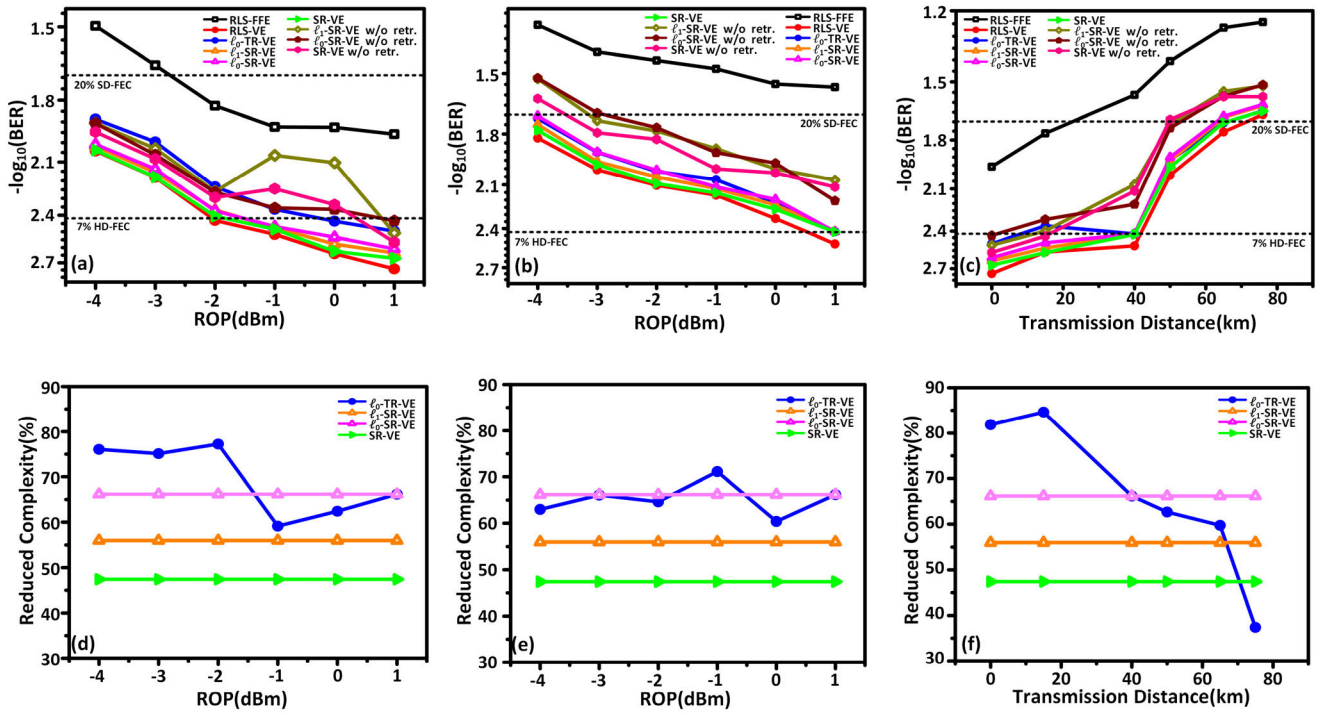

FIGURE 10. The measured BER performances of 150 Gbit/s PAM8 signal using different equalizers after (a) OBTB transmission and (b) 40km SSMF transmission. (c) BER performances of 150 Gbit/s PAM8 signal using different equalizers in terms of transmission distance. The reduced complexity percentage for different equalizers when the ROP varies after (d) OBTB transmission and (e) 40km SSMF transmission. (f) The reduced complexity percentage for different equalizers in terms of transmission distance.

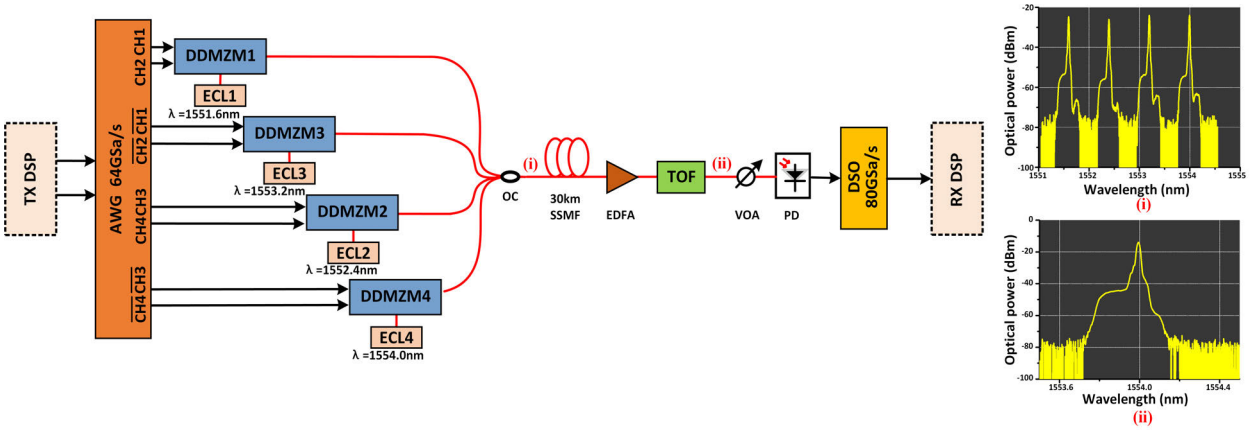

FIGURE 11. The experimental setup of 4 × 150 Gbit/s PAM8 signal transmission over 30 km SSMF using the proposed SR-VE.

their differential ports are used to modulate the optical sources with a wavelength of 1552.4 nm and 1554.0 nm, respectively. By this means, the modulated SSB-PAM8 signal on each adjacent two optical carriers are independent. Subsequently, these four modulated optical SSB-PAM8 signals are multiplexed by an optical coupler (OC). Insert (i) in Fig. 11 shows the optical spectrum of the transmitted optical signal after OC.

After 30 km SSMF propagation, the transmitted optical signal is amplified by an EDFA, and a TOF placed after this EDFA is used to filter out each Lane individually for performance evaluation. Insert (ii) in Fig. 11 presents the optical spectrum of the received optical signal in Lane4 after TOF. A VOA is used to adjust the ROP value. At last, the optical signal is detected by a PD, and then the detected electrical signal is captured by a DSO (LeCroy LabMaster 10-36Zi-A) operating at 80 GSa/s for the offline process. The full RLS-VE or sparse VEs are used to compensate for the linear and nonlinear distortion in the transmission link for comparison. About 1×10^5 bits are calculated for BER counting.

The measured BER performances of four-channel 150 Gbit/s PAM8 signal after 30 km SSMF transmission in terms of ROP are plotted in Fig. 12(a), (b), (c), and (d),

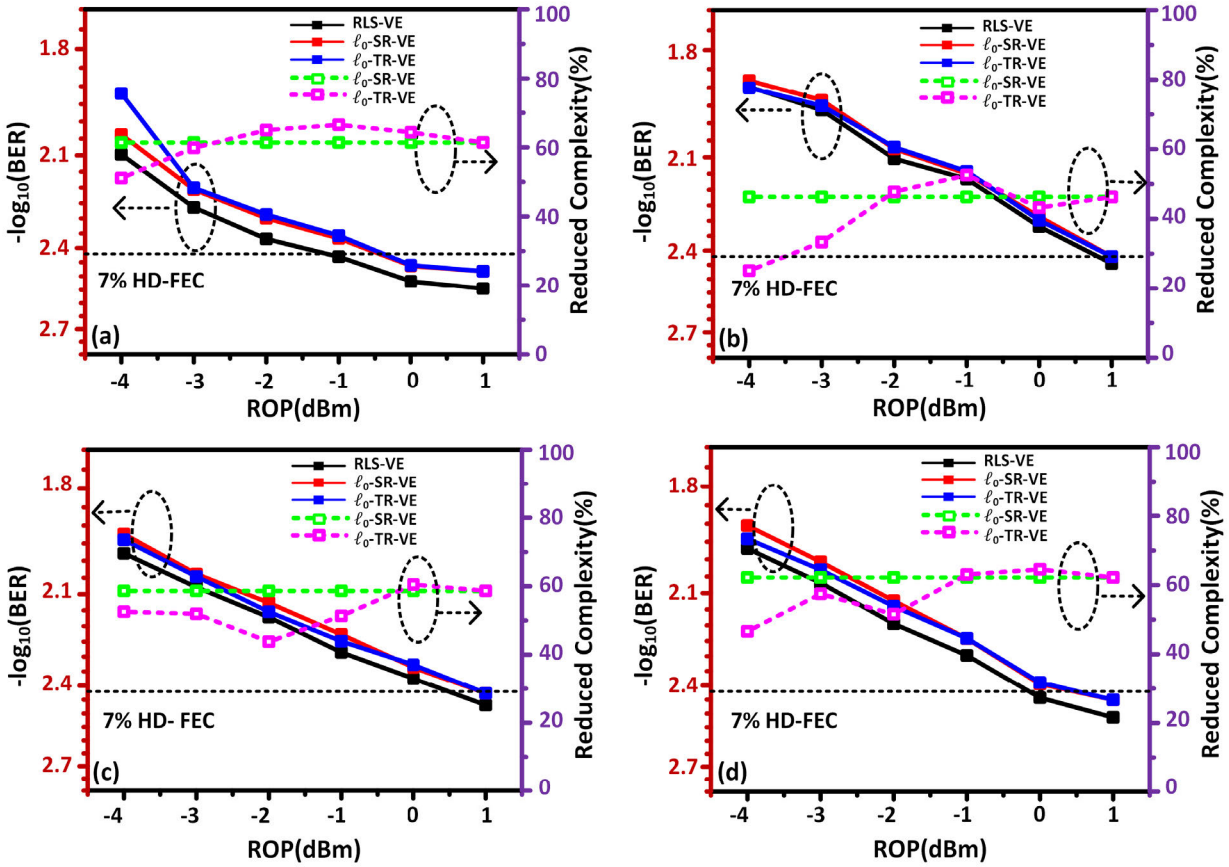

FIGURE 12. BER performances of 150 Gbit/s PAM8 signal using RLS-VE, ℓ_0-SR-VE and ℓ_0-TR-VE, and the reduced complexity percentage using ℓ_0-SR-VE and ℓ_0-TR-VE after 30 km SSMF transmission at Lane1 (a), Lane2 (b), Lane3 (c) and Lane4 (d).

respectively. Note that a full RLS-VE (111,19,15) is adopted in our experiment for all Lanes. Compared to the full RLS-VE, the reduced complexity percentage of ℓ_0-SR-VE and ℓ_0-TR-VE are also compared in Fig. 12(a)-(d). When the full RLS-VE is used, the measured receiver sensitivity at the HD-FEC threshold is -1 dBm, 0.8 dBm, 0.5 dBm, and -0.2 dBm for Lane1, Lane2, Lane3, and Lane4, respectively. Different power penalties for different lanes can be attributed to different characteristics of optical and electrical components. It could be observed in Fig. 12(a)-(d) that in all lanes, both ℓ_0-SR-VE and ℓ_0-TR-VE can effectively reduce the algorithm complexity at the expense of <0.5 dB power penalty compared to the full RLS-VE. Moreover, it is proven that the reduced complexity percentage variation of ℓ_0-TR-VE is >20%, but the proposed ℓ_0-SR-VE has stable computational complexity. However, the average reduced complexity percentage of the proposed ℓ_0-SR-VE is about 60% compared to the full RLS-VE even after 30 km SSMF transmission in all lanes.

V. CONCLUSION

With the help of VE, 150 Gbit/s PAM8 signal is experimentally transmitted over 40 km SSMF at C-band, and no CD compensation due to the use of DDMZM. To reduce the computational complexity of a three-order full RLS-VE, a robust RLS-based VE using ℓ_0-regularization is proposed. Compared to the full RLS-VE, the reduced complexity percentage of the proposed ℓ_0-SR-VE is 66.18% even after 75 km SSMF transmission in our experiment. Moreover, compared to the reported TR-VE, the computational complexity of the proposed ℓ_0-SR-VE only depends on its parameters but not the tap threshold, contributing to stable computational complexity. Based on this equalizer, 4 × 150 Gbit/s PAM8 signal has been successfully transmitted over 30 km SSMF at C-band without CD compensation. The reduced complexity percentage variation of ℓ_0-TR-VE is >20%, but the average reduced complexity percentage of the proposed ℓ_0-SR-VE is stable at 60% even after 30 km SSMF transmission in all lanes. These results predict that the proposed ℓ_0-SR-VE may have very practical value in high-speed short-reach applications.

ACKNOWLEDGMENT

(Wen Cheng and Haiping Song contributed equally to this work.)

REFERENCES

[1] Y. Gao, J. C. Cartledge, S. S.-H. Yam, A. Rezania, and Y. Matsui, "112 Gb/s PAM-4 using a directly modulated laser with linear pre-compensation and nonlinear post-compensation," in *Proc. Eur. Conf. Opt. Commun. (ECOC)*, Sep. 2016, pp. 1–3.

[2] H.-B. Zhang, N. Jiang, Z. Zheng, and W.-Q. Wang, "Experimental demonstration of FTN-NRZ, PAM-4, and duobinary based on 10-gbps optics in 100G-EPON," *IEEE Photon. J.*, vol. 10, no. 5, pp. 1–13, Oct. 2018.
[3] M. A. Mestre, H. Mardoyan, A. Konczykowska, R. Rios-Muller, J. Renaudier, F. Jorge, B. Duval, J.-Y. Dupuy, A. Ghazisaeidi, P. Jenneve, and S. Bigo, "Direct detection transceiver at 150-Gbit/s net data rate using PAM 8 for optical interconnects," in *Proc. Eur. Conf. Opt. Commun. (ECOC)*, Sep. 2015, pp. 1–3.
[4] F. Li, Z. Li, Q. Sui, J. Li, X. Yi, L. Li, and Z. Li, "200 Gbit/s (68.25 Gbaud) PAM8 signal transmission and reception for intra-data center interconnect," in *Proc. Opt. Fiber Commun. Conf. (OFC)*, Mar. 2019, pp. 1–3.
[5] M. Zhu, J. Zhang, S. Hu, X. Yi, B. Xu, M. Xiang, and K. Qiu, "Complexity reduction with a simplified MIMO volterra filter for PDM-Twin-SSB PAM-4 transmission," *J. Lightw. Technol.*, vol. 38, no. 4, pp. 769–776, Feb. 15, 2020.
[6] M. Zhu, J. Zhang, H. Ying, X. Li, M. Luo, X. Huang, Y. Song, F. Li, X. Yi, and K. Qiu, "56-Gb/s optical SSB PAM-4 transmission over 800-km SSMF using DDMZM transmitter and simplifified direct detection Kramers-Kronig receiver," in *Proc. Opt. Fiber Commun. Conf. (OFC)*, Mar. 2018, pp. 1–3.
[7] W. Wang, F. Li, Z. Li, Q. Sui, and Z. Li, "Dual-drive mach-zehnder modulator-based single side-band modulation direct detection system without Signal-to-Signal beating interference," *J. Lightw. Technol.*, vol. 38, no. 16, pp. 4341–4351, Aug. 15, 2020.
[8] L. Shu, J. Li, Z. Wan, F. Gao, S. Fu, X. Li, Q. Yang, and K. Xu, "Single-lane 112-Gbit/s SSB-PAM4 transmission with dual-drive MZM and Kramers–Kronig detection over 80-km SSMF," *IEEE Photon. J.*, vol. 9, no. 6, pp. 1–9, Dec. 2017.
[9] D. Li, H. Song, W. Cheng, L. Deng, M. Cheng, S. Fu, M. Tang, and D. Liu, "180 Gb/s PAM8 signal transmission in bandwidth-limited IMDD system enabled by tap coefficient decision directed volterra equalizer," *IEEE Access*, vol. 8, pp. 19890–19899, 2020.
[10] Z. Li, M. S. Erkilinc, K. Shi, E. Sillekens, L. Galdino, B. C. Thomsen, P. Bayvel, and R. I. Killey, "SSBI mitigation and the Kramers–Kronig scheme in single-sideband direct-detection transmission with receiver-based electronic dispersion compensation," *J. Lightw. Technol.*, vol. 35, no. 10, pp. 1887–1893, May 15, 2017.
[11] Z. Li, M. S. Erkilinc, K. Shi, E. Sillekens, L. Galdino, T. Xu, B. C. Thomsen, P. Bayvel, and R. I. Killey, "Digital linearization of direct-detection transceivers for spectrally efficient 100 Gb/s/λ WDM metro networking," *J. Lightw. Technol.*, vol. 36, no. 1, pp. 27–36, Jan. 1, 2018.
[12] C. Füllner, M. M. H. Adib, S. Wolf, J. N. Kemal, W. Freude, C. Koos, and S. Randel, "Complexity analysis of the Kramers-Kronig receiver," *J. Lightw. Technol.*, vol. 37, no. 17, pp. 4295–4307, Sep. 1, 2019.
[13] N.-P. Diamantopoulos, H. Nishi, W. Kobayashi, K. Takeda, T. Kakitsuka, and S. Matsuo, "On the complexity reduction of the second-order volterra nonlinear equalizer for IM/DD systems," *J. Lightw. Technol.*, vol. 37, no. 4, pp. 1214–1224, Feb. 15, 2019.
[14] N.-P. Diamantopoulos, W. Kobayashi, H. Nishi, K. Takeda, T. Kakitsuka, and S. Matsuo, "56-Gb/s VSB-PAM-4 over 80-km using 1550-nm EA-DFB laser and reduced-complexity nonlinear equalization," in *Proc. Eur. Conf. Opt. Commun. (ECOC)*, Sep. 2017, pp. 1–3.
[15] L. Ge, W. Zhang, C. Liang, and Z. He, "Threshold-based pruned retraining Volterra equalization for 100Gbps/lane and 100-m optical interconnects based on VCSEL and MMF," *J. Lightw. Technol.*, vol. 37, no. 13, pp. 3222–3228, Jul. 1, 2019.
[16] Y.-Y. Lin, C.-J. Chen, H.-M. Nguyen, C.-Y. Chuang, C.-C. Wei, J. Chen, and J.-W. Shi, "Reduction in complexity of volterra filter by employing ℓ_0-regularization in 112-Gbps PAM-4 VCSEL optical interconnect," in *Proc. Opt. Fiber Commun. Conf. (OFC)*, Mar. 2020, pp. 1–3.
[17] Q. Yu, Y. Wang, D. Li, H. Song, Y. Fu, X. Jiang, L. Huang, M. Cheng, D. Liu, and L. Deng, "Secure 100 Gb/s IMDD transmission over 100 km SSMF enabled by quantum noise stream cipher and sparse RLS-volterra equalizer," *IEEE Access*, vol. 8, pp. 63585–63594, 2020.
[18] D. Li, W. Cheng, H. Song, L. Deng, M. Cheng, S. Fu, M. Tang, and D. Liu, "C-band 4×150 Gbit/s PAM8 transmission over 30 km SSMF using direct detection without CD compensation," in *Proc. Conf. Lasers Electro-Opt.*, May 2020, pp. 1–3.
[19] Y. Gu, J. Jin, and S. Mei, "ℓ0 norm constraint LMS algorithm for sparse system identification," *IEEE Signal Process. Lett.*, vol. 16, no. 9, pp. 774–777, Sep. 2009.
[20] E. M. Eksioglu and A. K. Tanc, "RLS algorithm with convex regularization," *IEEE Signal Process. Lett.*, vol. 18, no. 8, pp. 470–473, Aug. 2011.
[21] N. Stojanovic, F. Karinou, Z. Qiang, and C. Prodaniuc, "Volterra and Wiener equalizers for short-reach 100G PAM-4 applications," *J. Lightw. Technol.*, vol. 35, no. 21, pp. 4583–4594, Nov. 1, 2017.

WEN CHENG received the M.S. degree in information and communication engineering from the Wuhan Research Institute of Posts and Telecommunications, Wuhan, China, in 2008. She is currently pursuing the Ph.D. degree with the Huazhong University of Science and Technology. In 2008, she joined FiberHome Technologies Group, as a Senior Engineer. Her research interests include fiber-optic communication and optical access networks.

HAIPING SONG received the B.S. degree in optoelectronics information science and engineer from Nanchang University, Nanchang, China, in 2017. He is currently pursuing the Ph.D. degree in optical engineering with the Huazhong University of Science and Technology, Wuhan, China. His research interests include optical interconnects networks and design of analog optical transceiver module.

DI LI received the B.S. degree in optical information engineering from the Huazhong University of Science and Technology (HUST), Wuhan, China, in 2016. He passed the test for Joint Master and Ph.D. program and was enrolled as a doctoral candidate at HUST, in 2017. He is currently pursuing the Ph.D. degree in optical engineering, HUST. His research interests includes optical fiber communication, including passive optical networks and short-reach applications.

PIN YI received the B.E. degree in optoelectronics information science and engineering from Tianjin University, Tianjin, China, in 2018. He is currently pursuing the M.S. degree in optical engineering with the Huazhong University of Science and Technology, Wuhan, China. His research interest includes digital signal processing in coherent optical fiber communication.

MENGFAN CHENG received the B.S. degree in information engineering, and the M.S. and Ph.D. degrees in computer science from the Huazhong University of Science and Technology, Wuhan, China, in 2005, 2007, and 2012, respectively. He is currently a Lecturer with the Huazhong University of Science and Technology. His research interests include secure communications, chaotic encryption, and chaotic synchronization.

DEMING LIU was born in Hubei, China, in January 1957. He received the degree from the Chengdu Institute of Telecommunication (University of Electronic Science and Technology of China), Chengdu, China, in 1984. He is currently a Professor with the Huazhong University of Science and Technology, Wuhan, China. His research interests include optical access networks, optical communication devices, and fiber-optic sensors.

LEI DENG received the B.S., M.S., and Ph.D. degrees from the Huazhong University of Science and Technology (HUST), Wuhan, China, in 2006, 2008, and 2012, respectively, all in optoelectronics and information engineering. From 2010 to 2012, he was with the Technical University of Denmark, as a Guest Ph.D. Student. He is currently a Professor with the School of Optical and Electronic Information, HUST. His research interests include fiber-optic communications, advanced modulation formats and OFDM in radio-over-fiber (RoF) systems, and next generation passive optical network systems.